Estimates of the Global Water Budget and Its Annual Cycle Using Observational and Model Data

KEVIN E. TRENBERTH, LESLEY SMITH, TAOTAO QIAN, AIGUO DAI, AND JOHN FASULLO

National Center for Atmospheric Research, Boulder, Colorado*

(Manuscript received 13 April 2006, in final form 2 October 2006)

ABSTRACT

A brief review is given of research in the Climate Analysis Section at NCAR on the water cycle. Results are used to provide a new estimate of the global hydrological cycle for long-term annual means that includes estimates of the main reservoirs of water as well as the flows of water among them. For precipitation P over land a comparison among three datasets enables uncertainties to be estimated. In addition, results are presented for the mean annual cycle of the atmospheric hydrological cycle based on 1979–2000 data. These include monthly estimates of P, evapotranspiration E, atmospheric moisture convergence over land, and changes in atmospheric storage, for the major continental landmasses, zonal means over land, hemispheric land means, and global land means. The evapotranspiration is computed from the Community Land Model run with realistic atmospheric forcings, including precipitation that is constrained by observations for monthly means but with high-frequency information taken from atmospheric reanalyses. Results for $E - P$ are contrasted with those from atmospheric moisture budgets based on 40-yr ECMWF Re-Analysis (ERA-40) data. The latter show physically unrealistic results, because evaporation often exceeds precipitation over land, especially in the Tropics and subtropics.

1. Introduction

Driven mainly by solar heating, water is evaporated from ocean and land surfaces, transported by winds, and condensed to form clouds and precipitation that falls to land and oceans. Precipitation over land may be stored temporarily as snow or soil moisture, while excess rainfall runs off and forms streams and rivers, which discharge the freshwater into the oceans, thereby completing the global water cycle (Fig. 1). Associated with this water cycle, energy, salt within the oceans, and nutrients and minerals over land are all transported and redistributed within the earth climate system (Chahine 1992; Schlesinger 1997). Thus, water plays a crucial role in earth's climate and environment.

Most studies of the global water cycle deal with only some specific aspects. There are also many regional or basin-scale synthesized analyses of the surface water budget, as reliable data are often available only over certain regions. Relatively few studies (e.g., Chahine 1992; Oki 1999) have attempted to provide a synthesized, quantitative view of the global water cycle, and our quantitative knowledge of the various components and their variability of the global water cycle is still fairly limited because of a lack of reliable data for surface evaporation, oceanic precipitation, terrestrial runoff, and several other fields.

A goal for our research is to put together a much more integrated and complete picture of all of the elements in the global water cycle, exploiting many different datasets and trying to take advantage of their merits while overcoming their deficiencies. To do this we make maximum use of physical constraints inherent in a closed budget, and physical models to help estimate components that are not well observed, such as evapotranspiration. In the following, the references are mainly those associated with our group at the National Center for Atmospheric Research (NCAR) and are not intended to be comprehensive (however, see the referenced papers for more complete context).

For the most part, the main hydrological cycle components have been studied in isolation. Major efforts

* The National Center for Atmospheric Research is sponsored by the National Science Foundation.

Corresponding author address: Kevin E. Trenberth, National Center for Atmospheric Research, P.O. Box 3000, Boulder, CO 80307-3000.
E-mail: trenbert@ucar.edu

DOI: 10.1175/JHM600.1

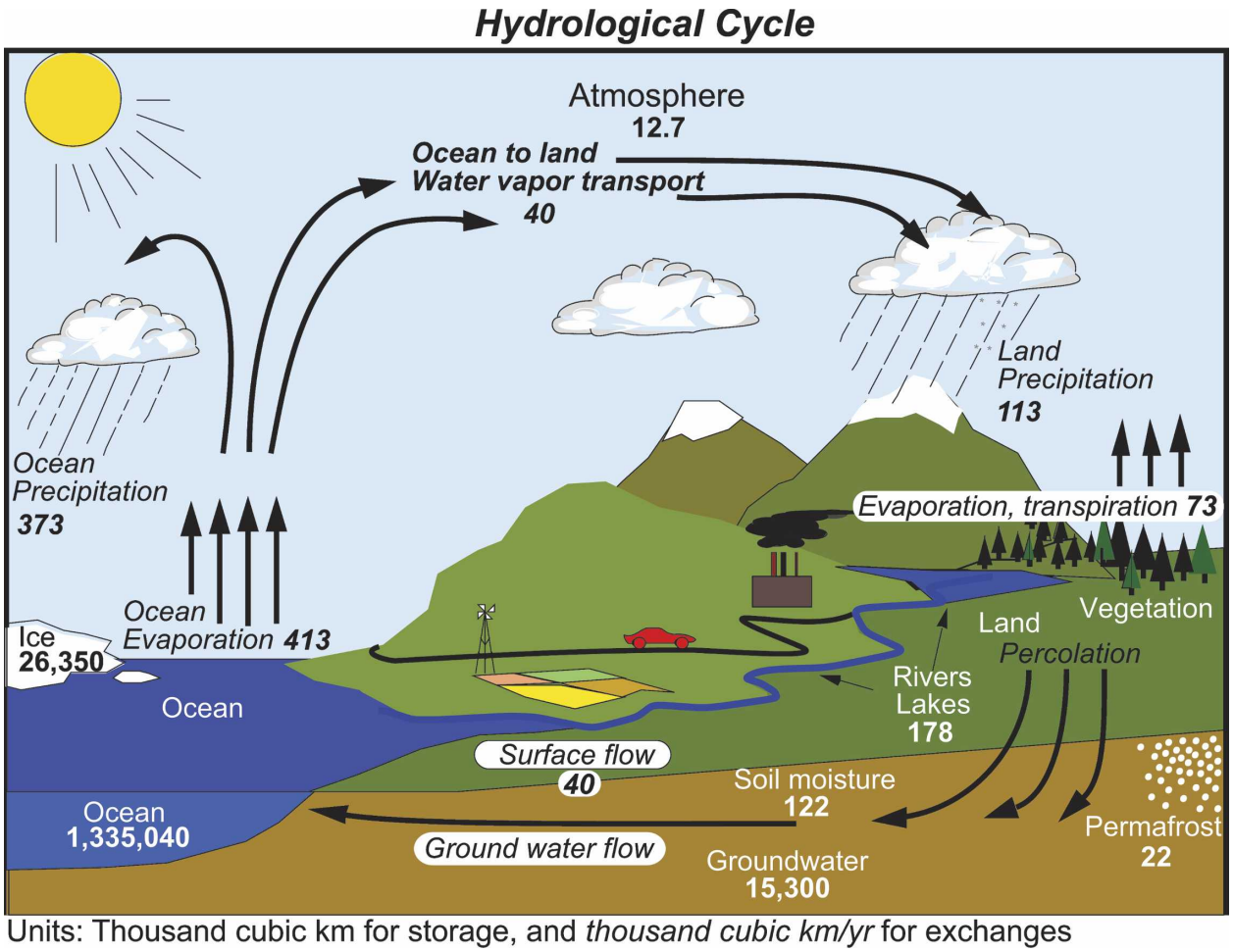

FIG. 1. The hydrological cycle. Estimates of the main water reservoirs, given in plain font in 10^3 km^3, and the flow of moisture through the system, given in slant font (10^3 km^3 yr^{-1}), equivalent to Eg (10^{18} g) yr^{-1}.

have been made to assemble, analyze, derive, and assess global datasets of water vapor (Trenberth et al. 2005), cloud (Dai et al. 1999b, 2006), precipitation (amount, frequency, intensity, type) (Trenberth 1998; Dai et al. 1999a; Dai 2001a; Trenberth et al. 2003), evapotranspiration (evaporation plus transpiration from plants) (Qian et al. 2006), soil moisture, runoff, streamflow and river discharge into the oceans (Dai and Trenberth 2002, 2003), atmospheric moisture flows and divergence (Trenberth and Guillemot 1998; Dai and Trenberth 2002; Trenberth and Stepaniak 2003a), atmospheric moisture storage (Trenberth and Smith 2005), and freshwater flows in the ocean (Dai and Trenberth 2003). Related issues are the effects of temperature and water-holding capacity, relative versus specific humidity (Dai 2006), covariability of temperature and precipitation (Trenberth and Shea 2005), recycling of moisture (which is taken to mean the fraction of precipitation in a given region, such as a river basin, that comes from moisture evaporated within that basin as opposed to advected in from outside the region) (Trenberth 1999), combinations of temperature and precipitation such as in the Palmer drought severity index (PDSI) (Dai et al. 2004), the diurnal cycle (Dai et al. 1999a,b; Dai 2001b; Trenberth et al. 2003), and forcings of the hydrological cycle, such as solar radiation (Qian et al. 2006). It is well established that latent heating in the atmosphere dominates the structural patterns of total diabatic heating (Trenberth and Stepaniak 2003a,b) and thus there is a close relationship between the water and energy cycles in the atmosphere.

Water vapor is the dominant greenhouse gas (Kiehl and Trenberth 1997) and is responsible for the dominant feedback in the climate system (Karl and Trenberth 2003). However, it also provides the main resource for clouds and storms to produce precipitation, and most precipitation comes from moisture already in the atmosphere at the time a storm forms (Trenberth

1998, 1999; Trenberth et al. 2003). Hence as global warming progresses, temperatures in the troposphere increase (Karl and Trenberth 2003) along with the water-holding capacity (governed by the Clausius–Clapyron equation), and so do actual water vapor amounts (Trenberth et al. 2005; Soden et al. 2005). The strong relationships with sea surface temperatures (SSTs) allow estimates of column water vapor amounts since 1970 to be made and results indicate increases of about 4% over the global oceans, suggesting that water vapor feedback has led to a radiative effect of about 1.5 W m^{-2} (Fasullo and Sun 2001), comparable to the radiative forcing of carbon dioxide increases (Houghton et al. 2001). This provides direct evidence for strong water vapor feedback in climate change.

The observed increase in atmospheric moisture in turn increases moisture convergence into storms (given the same low-level atmospheric convergence), and thus increases intensity of precipitation, as observed (Trenberth 1998; Trenberth et al. 2003), while frequency and duration are apt to decrease, exacerbating drought. This comes about because the total precipitation amount is constrained by the available surface energy and how much goes into evaporation. Hence, enhanced intensity implies reduced frequency or duration if the amount is the same. Drought appears to have increased substantially globally since the 1970s (Dai et al. 2004) in part because of decreased precipitation over land (mainly in the Tropics and subtropics) but also because of warming and increased atmospheric demand for moisture. Drought has increased especially throughout Africa, southern Asia, the southwestern United States, and the Mediterranean region (both southern Europe and northern Africa), and has also influenced the Amazon, while precipitation has increased at higher latitudes in Europe, northern Asia, North America, and South America (Dai et al. 2004) in part because higher temperatures increase water-holding capacity and more precipitation falls as rain instead of snow (Trenberth and Shea 2005).

A longstanding challenge is to provide a reliable estimate of the annual mean global water cycle. Our latest estimate is given in Fig. 1 and, while there are large uncertainties in many of the estimated numbers, section 3 documents the sources of information and new results that have been included. An ongoing challenge is to better determine these values. Most likely, this can be addressed by examining the variability on several time scales. In particular, a second challenge, taken up in section 4, is to determine the annual cycle of the global mean water cycle, and an attempt is given here for some parts of this, namely, the atmospheric branch. The annual cycle is pronounced because of the asymmetry of land between the two hemispheres. Therefore, there is a need to resolve continental scales and zonal mean latitude–time sections, and these results are also presented in section 4. The third challenge posed is to determine the interannual and longer-term variability of this cycle. This is especially an issue with nonstationary components associated with global climate change. For the most part, this aspect is taken up elsewhere.

The methods and most datasets used in sections 3 and 4 are discussed in section 2. In addressing some of the challenges, we also briefly comment on the quality of some of the datasets. In particular, we have three global land precipitation datasets that can be compared. We have also performed extensive diagnostics using 40-yr European Centre for Medium-Range Weather Forecasts (ECMWF) Re-Analysis (ERA-40) data, but we limit how many of these are presented because of problems that will become apparent. The conclusions are given in section 5.

2. Methods and data

There are known problems with the National Oceanic and Atmospheric Administration's (NOAA's) Climate Prediction Center (CPC) Merged Analysis of Precipitation (CMAP) (Xie and Arkin 1997) over the oceans, especially for trends (Yin et al. 2004), and thus for precipitation P we prefer to use the newer version 2 of the Global Precipitation Climatology Project (GPCP) data (Adler et al. 2003) that are a blend of satellite and gauge data and provide global coverage. We also make use of two other land precipitation datasets. The University of East Anglia Climatic Research Unit (CRU) TS 2.1 land precipitation dataset is from Mitchell and Jones (2005). The PREC/L dataset is from Chen et al. (2002) and includes both Global Historical Climatology Network (GHCN) and synoptic data from NOAA/CPC's Climate Anomaly Monitoring System (CAMS). Adam and Lettenmaier (2003) and Adam et al. (2006) discuss precipitation undercatch biases over land, especially for snow, and errors of interpolation in areas of steep and complex topography combined with biases in observing site locations that are likely present in these datasets to some extent. Annual precipitation for the circumpolar region north of 50°N has increased during the past 50 yr by approximately 4% but this increase has not been homogeneous in time and space (Groisman et al. 2005). Hence undercatch has changed over time because more snow falls as rain as the climate warms. The Parameter-Elevation Regressions on Independent Slopes Model (PRISM)

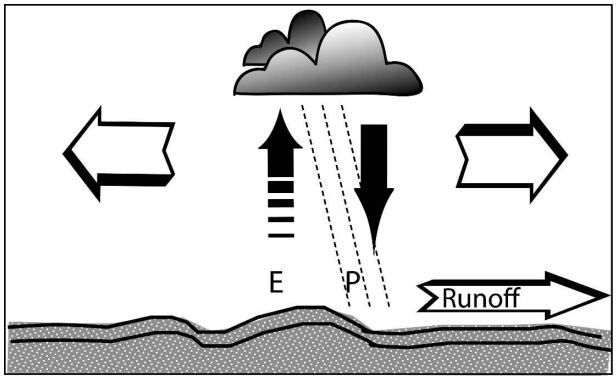

FIG. 2. Schematic of the local atmospheric water balance. The large arrows indicate atmospheric moisture divergence, which is mostly compensated for by evapotranspiration E and precipitation P, as changes in atmospheric moisture storage are small. At the surface $E - P$ is balanced by surface and subsurface runoff, and changes in soil moisture and groundwater.

(Daly et al. 2002) used an elevation model to account for slopes and their orientation to the winds and therefore includes an adjustment for orographic bias, giving precipitation at 5′ resolution, but this is not available globally.

To examine the regional hydrological cycle and its annual cycle, we use several datasets to compute the same quantities and this also serves as a validation of reanalysis results. The seasonal variation of E over land is taken from a stand-alone integration of the Community Land Model version 3 (CLM3) (Bonan et al. 2002; Qian et al. 2006). The CLM3 is a substantial improvement over previous versions of land surface models and represents the surface with five primary subgrid land cover types, 16 plant functional types, and 10 layers for soil temperature and water, with explicit treatment of liquid soil water and ice. Representation of the seasonal cycle by the CLM3 shows significant improvements over previous generation models in surface air temperature, snow cover, and runoff (Bonan et al. 2002; Dickinson et al. 2006). In the stand-alone integration used here, the CLM3 was forced with observed monthly precipitation and other fields blended with high-frequency weather information from the National Centers for Environmental Prediction (NCEP)–NCAR reanalysis (Qian et al. 2006). Values are reported on a T42 grid (~2.8°), on a monthly basis from 1948 to 2004. The precipitation dataset is a blend of PREC/L and GPCP to ensure complete coverage.

The $E - P$ has been computed from the moisture budget from ERA-40 (Uppala et al. 2005), as in Trenberth and Guillemot (1998) for NCEP–NCAR reanalyses and schematically illustrated in Fig. 2. We define **Q** as the total column vector flux of moisture. We also estimate $E - P$ using the CLM3 estimate of E and the observed P, and compare with ERA-40 results. ERA-40 data are also used to provide estimates of mean changes in the atmospheric storage of water vapor, which can be significant with the annual cycle (Trenberth and Smith 2005). Note that Trenberth et al. (2005) have found substantial problems in the ERA-40 precipitable water values in the low latitudes in particular, and this has led to a hydrological cycle that is too vigorous (Uppala et al. 2005). We confirm these problems and document them in more detail as well.

3. The global hydrological cycle

The long-term mean global hydrological cycle as depicted in Fig. 1 is uncertain in several respects. Various versions of it have been published before, usually without any statements of source or the origins of the values assigned to the various reservoirs or the fluxes through the system. Tracing some of the references also indicates a cascade whereby one source cites another that in turn cites another and the original value is often not very certain. Dozier (1992) presents a version of the hydrological cycle but the values predate the mid-1980s. Chahine (1992) also provides a review of the hydrological cycle and has another version, as does Schlesinger (1997), based in part on the Chahine version, and this in turn has been used by Alley et al. (2002). The most comprehensive listings of many tables of relevant data are given by Gleick (1993), who notes that "good water data are hard to come by" and that the data are "collected by individuals with differing skills, goals, and intents." In the same volume, Shiklomanov (1993) compiles what remains the most definitive set of values for the water reserves on earth and he also estimates the water balance, and thus much of what goes into the overall hydrological cycle. Many of his values in turn come from Korzun (1978) and Baumgartner and Reichel (1975). Shiklomanov and Rodda (2003) provide an updated discussion but most of the values for the global hydrological cycle are identical to those in the 1993 article. The exception is a slightly different partitioning of the evaporation between land and ocean. Peixoto and Oort (1992) also provide an estimated global water cycle based in part on their computations for atmospheric transports. A more recent compilation is by Oki (1999), based on newer estimates of atmospheric transports from ECMWF and precipitation data from earlier versions of CMAP for 1989–92.

As noted above, there are known problems with CMAP oceanic precipitation, and thus for precipitation P we use the GPCP version 2 data. For Fig. 1 we take

the mean values from only 1988 to 2004, as the post-1987 data benefit from the microwave data from the Special Sensor Microwave Imager (SSM/I) and other sources. The annual mean global GPCP values are $486.9 \pm 2.9 \times 10^3$ km^3, where we used twice the standard error of the annual means over the 17 yr to compute the temporal sampling variability error. In the following, the units are 10^3 km^3 yr^{-1} to enable monthly values to be compared to the annual mean. Over the global ocean, GPCP precipitation features an annual cycle with peak values of 381.2 units in October, a minimum in June of 365.0, and annual mean of 372.8 ± 2.7. Over land, the annual mean GPCP value is 112.6 ± 1.4 units and the mean annual cycle peaks in July at 127.9 and with a minimum in February of 104.7. There is a strong inverse relationship between land and ocean precipitation in the annual cycle, which is also apparent in the interannual variability (Curtis and Adler 2003).

Over land we can compare the GPCP values with those from CRU and PREC/L for 1988 to 2004. All three datasets feature the same months as having maximum and minimum mean values, except that PREC/L has a minimum in November comparable to that in February. For CRU the annual mean is 109.5 ± 1.3, although this excludes Antarctica, and for PREC/L it is 111.2 ± 1.1 units, versus our GPCP value of $112.6 \pm 1.4 \times 10^3$ km^3. Hence the GPCP values are highest of the three, most likely because of a correction that was applied for undercatch using climatological coefficients. The other global studies had land precipitation as 115 units (Oki 1999), 107 (Chahine 1992), 99 (Peixoto and Oort 1992), and 110 (Shiklomanov 1993). Except for the Peixoto and Oort (1992) value, these are all reasonably close, given the different time periods considered.

Over the ocean, our GPCP precipitation of $372.8 \pm 2.7 \times 10^3$ km^3 can be compared with earlier global studies which had 391 (Oki 1999), 398 (Chahine 1992), 324 (Peixoto and Oort 1992), and 458 units (Shiklomanov 1993). The latter is far too high by 23% and the value of Peixoto and Oort (1992) is too low by 13%.

Adam and Lettenmaier (2003) estimate that uncorrected land precipitation may suffer from gauge-undercatch biases of 11.7%. Furthermore, the nonrepresentative locations where gauges are located can lead to errors of interpolation in areas of steep and complex topography that could induce an underestimate of 6.2% for global land precipitation (Adam et al. 2006). The two biases could amount to a total deficiency bias of 17.9% of global terrestrial annual mean precipitation (excluding Antarctica). However, this bias estimate is dataset dependent (Adam et al. 2006). For example, the orography-related bias in the PREC/L dataset is likely to be smaller than in other datasets because of its use of a very large network of gauges in creating the monthly climatology from which anomalies for individual months were derived and gridded (Chen et al. 2002). We have not attempted to apply any corrections to the precipitation data, although new daily precipitation data for the northern high latitudes with corrections of the gauge-undercatch (but not orography) biases have recently become available (Yang et al. 2005). This is also why the GPCP land data may be less biased, albeit only slightly compared with the PREC/L. The temporal sampling uncertainty error bars are comparable to the differences in mean values between the different datasets. However, the range among the three recent datasets for global land is only 3%, and this drops to less than 2% if Antarctica is factored out. The range becomes larger if other periods are considered, however.

Ice volumes of 28.74×10^6 km^3 are taken from Houghton et al. (2001) and include glaciers, ice caps, and ice sheets, and values are used with a 0.917 density factor to convert to liquid water equivalent in Fig. 1. Ohmura (2004) provides an alternative assessment but the reliability of some values is questionable. In the past, the volume of Antarctica has often been overestimated, for instance. For permafrost or ground ice, values are quite uncertain. Permafrost occupies about 24% of the land surface in the Northern Hemisphere and Ohmura (2004) estimates a value of 400×10^3 km^3. Zhang et al. (1999) suggest a range from 11.4 to 36.6×10^3 km^3 as the "excess ground ice," and including the pore ground ice would make the total volume much larger (190 to 290×10^3 km^3; T. Zhang 2006, personal communication). The ice volume from Zhang et al. (1999) better represents permafrost, and the water equivalent is 10.4 to 33.5×10^3 km^3, so that for Fig. 1 we choose a central value of 22×10^3 km^3. For soil moisture we use the estimate of 121 800 km^3 from Webb et al. (1993), and for groundwater we take values from Schlesinger (1997). The ocean volume is estimated from the updated National Geophysical Data Center terrain database with global 5-min ocean depth (and land elevation) data to be 1.33504×10^9 km^3. In the past this has generally been overestimated as 1.4×10^9 km^3 (Chahine 1992), or about 1.35×10^9 km^3 in Peixoto and Oort (1992) and several other studies. Atmospheric water vapor amounts (12.7×10^3 km^3) are from Trenberth and Smith (2005) and we are able to refine the value to an extra decimal place. Most previous estimates were about 13×10^3 km^3 although Chahine (1992) quoted an excessively high value of 15.5×10^3 km^3.

River discharge into the ocean is based on the comprehensive analysis of Dai and Trenberth (2002), which found a river discharge of 37.3×10^3 km^3, although that excluded estimates from Antarctica. As noted by Dai and Trenberth (2002), an estimate of the Antarctic contribution is 2.6×10^3 km^3 giving a total runoff into the ocean of 40.0×10^3 km^3. Other small contributions may come from discharge into inland seas. This value is surprisingly close to some previous estimates and identical to that of Oki (1999). Shiklomanov (1993) gave a value of 42.6×10^3 km^3, presumably based on Baumgartner and Reichel (1975); Chahine (1992) suggested 36×10^3 km^3; and Peixoto and Oort (1992) estimated 37×10^3 km^3.

In Fig. 1, evapotranspiration E has been computed as a residual of the precipitation and runoff values to give 72.6×10^3 km^3. We have also computed evapotranspiration from precipitation and atmospheric moisture budgets (Fig. 2) that give $E - P$ estimates (e.g., Trenberth and Guillemot 1998; Trenberth et al. 2001), but these have to be reconciled with runoff and river discharge data (Dai and Trenberth 2002). Below we examine the latest estimates of $E - P$ from ERA-40 in more detail. In addition, as detailed in section 4, new estimates of global evapotranspiration have been computed and global results suggest values as low as 67×10^3 km^3 for annual means over 1979–2000 (during which time the land precipitation was also lower at 108×10^3 km^3). In the CLM3 results, the runoff is smaller than in Dai and Trenberth (2002) in low latitudes, but somewhat higher in high latitudes. Some differences also arise from the use of the different periods [e.g., the CLM3 simulations suggest that the runoff is 40.4×10^3 km^3 yr^{-1} (1979–2000) but 41.8×10^3 km^3 yr^{-1} (1948–2004)].

Indeed, many of these values are not constant, owing to climate change, as noted above. Nor is it possible to place reliable error bars on many of the quantities, so that uncertainties remain. We have at least documented the heritage of the values assigned here and they are based on much better and more complete data than the earlier estimates cited above. In the above we have given comparisons from earlier works in the places where we have derived new values in Fig. 1. Some values, such as land precipitation, have not changed much, but ocean precipitation has, and so too therefore have the corresponding evaporation estimates. The overall transport of moisture from ocean to land has converged in recent estimates to be a little higher than in Peixoto and Oort (1992) but the 7% differences are the same order as those into Antarctica, and hence depend on the accuracies of the Antarctica exchanges.

4. Annual cycle results

a. $E - P$

The ERA-40 data have been used to compute all the terms in the atmospheric moisture budget on a monthly basis, and the annual mean for 1979 to 2001 $E - P$ is given in Fig. 3. The strong evaporation in the subtropics over the oceans is readily apparent ($E > P$) and so too is the tropical intertropical convergence zones and monsoon rains, where $P > E$. This figure nicely shows the main characteristics of the $E - P$ field, but the values cannot be considered quantitatively correct, as discussed below. Over land it is generally expected that $P > E$, because runoff is positive, although exceptions can arise if water is transported into a region from rivers or aqueducts, or if major lakes exist. In this figure, values close to zero are not contoured and do not therefore allow small negative values to be seen, but positive $E - P$ that is clearly not physical exists in parts of South America, Africa, and perhaps Asia, although the latter spot is near the Caspian Sea. In fact, $E - P$ values are positive in most months over Australia and other parts of the Tropics (see Fig. 8 shown later), and hence we do not show them in the figure and nor do we use these values for the main assessment in section 3.

b. Atmospheric annual cycle

To overcome the ERA-40 problems, we instead use the results for the period 1979–2000 from the CLM3 historical model simulations forced with the specified observed precipitation and other atmospheric forcings, and the CLM3 model computed the evapotranspiration and runoff. We do not make use of the latter here, as human interference and withdrawal are outstanding issues, although surface moisture balance and runoff are being pursued in other studies. We use changes in atmospheric storage of moisture ΔS from ERA-40 [see Trenberth and Smith (2005) for cross checks on these amounts], and then compute the atmospheric moisture divergence as a residual $\nabla \cdot \mathbf{Q} = E - P - \Delta S$ for each continent, and for land as a whole. Figures 4 to 6 summarize the features of the seasonal cycle for the globe, land areas in each hemisphere, and continents.

The presentations use bars to present the monthly mean and annual mean values, with P as the top of the solid colors, E as blue, the atmospheric moisture convergence $-\nabla \cdot \mathbf{Q}$ as green, and the change in atmospheric storage ΔS as red. Hence, $P = E - \nabla \cdot \mathbf{Q} - \Delta S$. Thus what is plotted as solid colors are the evaporation, convergence of moisture, and decreases in the change in storage. Values are cross hatched where they take moisture away from precipitation in the moisture budget, for instance, by indicating instead an increase in

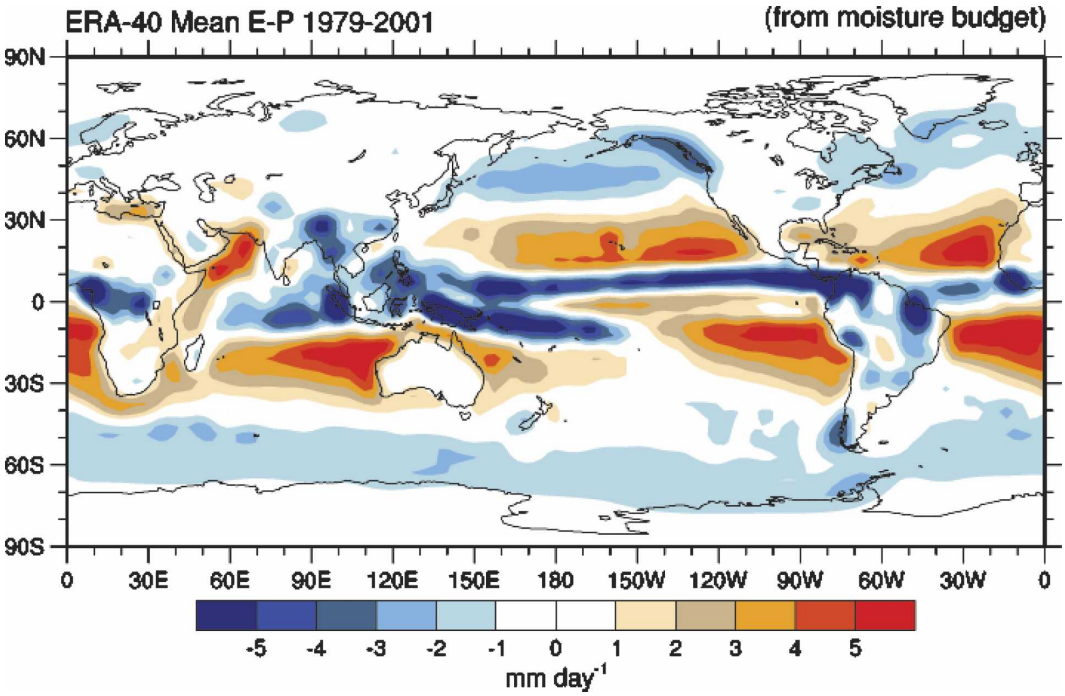

FIG. 3. The long-term 1979–2001 annual mean $E - P$ computed from monthly means of the vertically integrated atmospheric moisture budget using ERA-40 reanalyses every 6 h.

moisture in the atmosphere. The units are Eg (10^{18} g). For global land (Fig. 4) both precipitation and evapotranspiration peak in July. The latter is limited in many areas by availability of surface moisture, but also depends on available energy, and both peak in July owing to the dominance of land in the Northern Hemisphere (NH). Atmospheric moisture convergence over land, however, peaks in January, in northern winter. Mois-

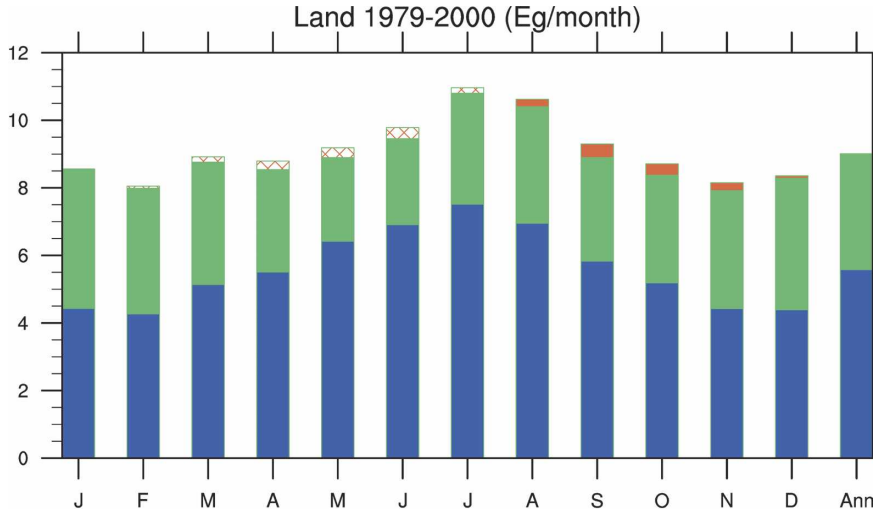

FIG. 4. Annual cycle of moisture budget for global land, (Eg month^{-1}) for 1979–2000. Given are the mean evaporation (blue), inferred column-integrated convergence of atmospheric moisture (green), minus the change in atmospheric storage (red) and total precipitation P as the sum of these $P = E - \nabla \cdot \mathbf{Q} - \Delta S$ at the top of the solid colors. Values that take moisture away from precipitation are cross hatched. The annual mean is given at right (multiply by 12 to get annual value).

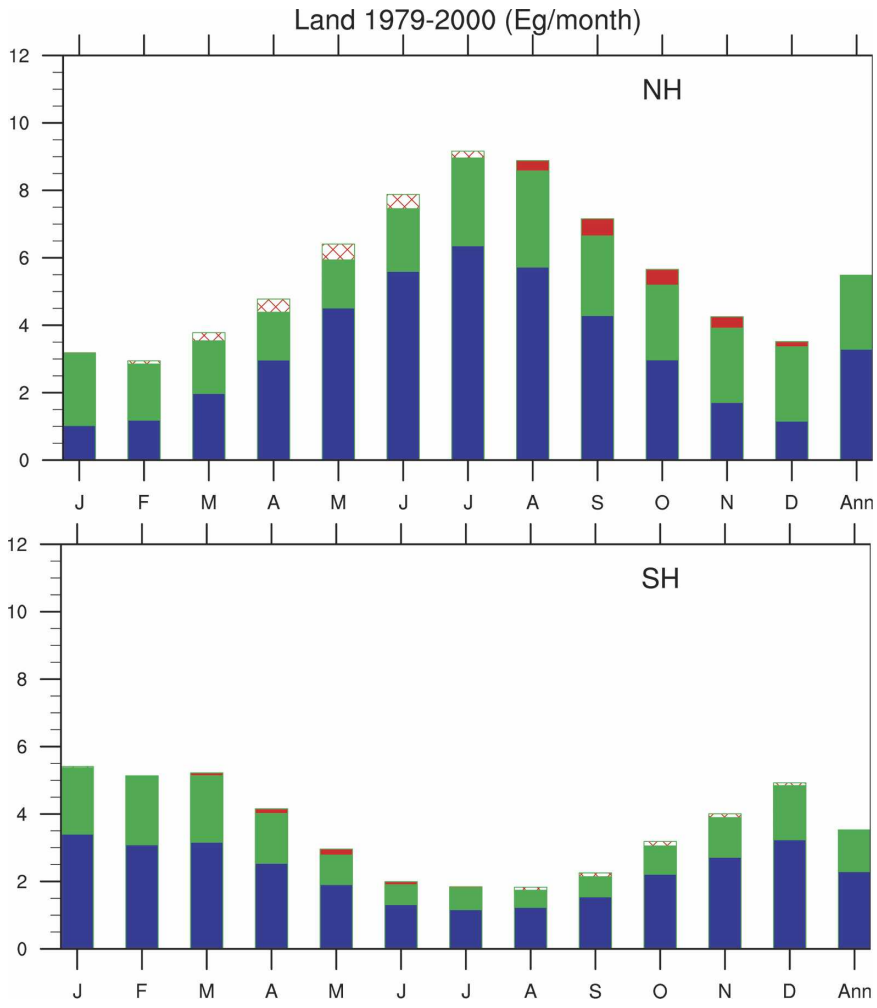

FIG. 5. Mean annual cycle of the moisture budgets over land for the (top) NH and (bottom) SH in Eg month^{-1} for 1979–2000. Given are the mean evaporation (blue), inferred column-integrated convergence of atmospheric moisture (green), minus the change in atmospheric storage (red) and total precipitation P at the top of the solid colors. Values that take moisture away from precipitation are cross hatched. The annual mean is given at right (multiply by 12 to get annual value).

ture storage in the atmosphere increases to peak in July as northern temperatures rise.

The breakdown into the hemispheric contributions (Fig. 5) brings out the seasonality much more clearly. It reveals the strong seasonality in the NH, with a minimum in precipitation and evaporation in January or February, when temperatures are lowest and thus water-holding capacity of the atmosphere is limiting. Meanwhile values are highest in the Southern Hemisphere (SH) in the southern summer in January, February, and March. However, the moisture convergence onto land in the NH undergoes only a very small annual cycle. Lowest values occur in February, March, April, and May, when SSTs are lowest, of about 1.8 Eg, increasing to about 3.0 Eg in August. In contrast, in the SH, convergence decreases along with precipitation and evaporation in winter, and is also a maximum in summer.

Figure 6 presents the values for the major continents or landmasses, with Europe and Asia combined. In North America, winter precipitation is overwhelmingly dominated by moisture convergence, while the latter is small in summer, and recycling of evaporated moisture is much more important (Trenberth 1999). The annual cycle is much larger in Eurasia in precipitation and evaporation, while it is here that the springtime moisture convergence is modest. Africa straddles the equator and has a weak annual cycle, as seasonal components in each hemisphere compensate, with moisture convergence always weak, and evaporation limited by

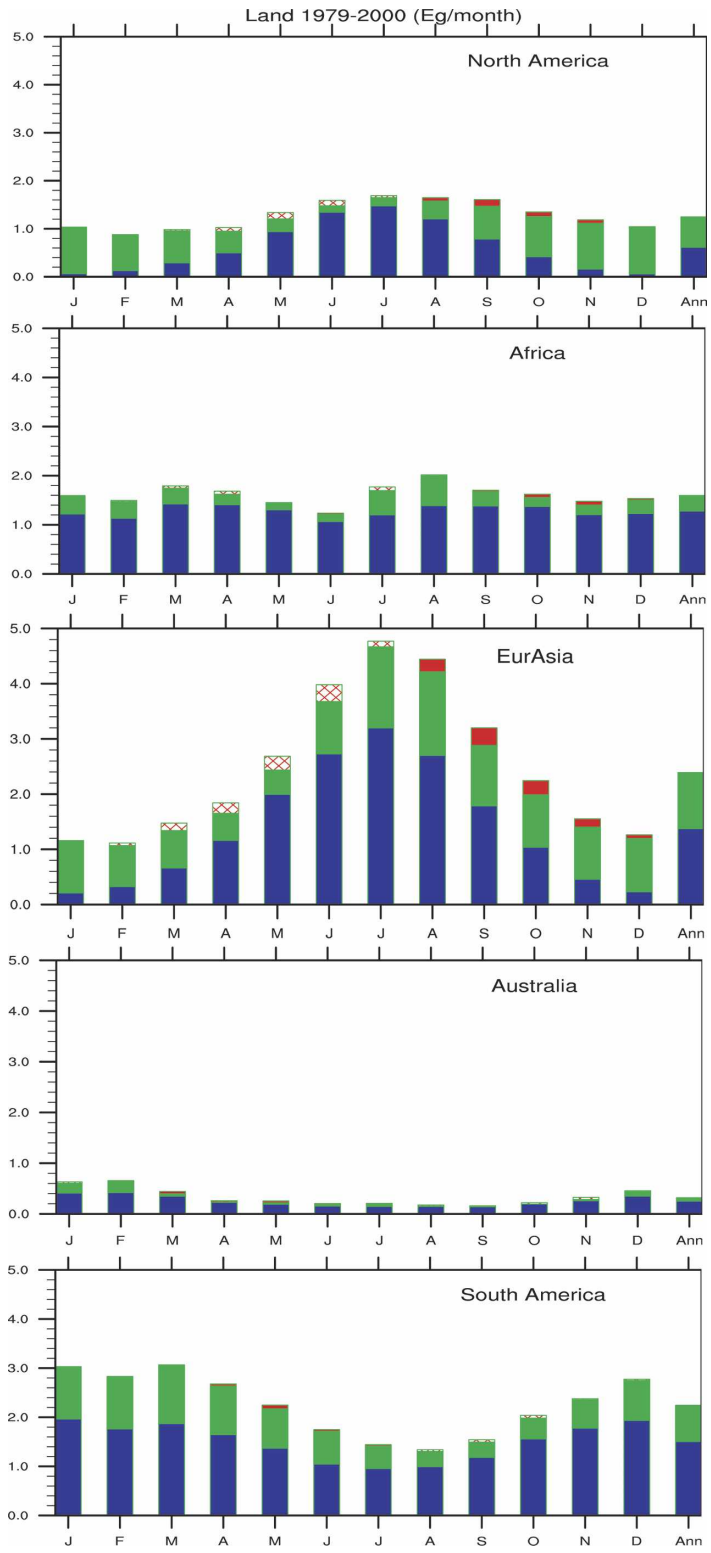

FIG. 6. Mean annual cycle of the moisture budgets for North America, Africa, Eurasia, Australia, and South America (Eg month^{-1}) for 1979–2000. Given are the mean evaporation (blue), inferred column-integrated convergence of atmospheric moisture (green), minus the change in atmospheric storage (red) and total precipitation P at the top of the solid colors. Values that take moisture away from precipitation are cross hatched. The annual mean is given at right (multiply by 12 to get annual value).

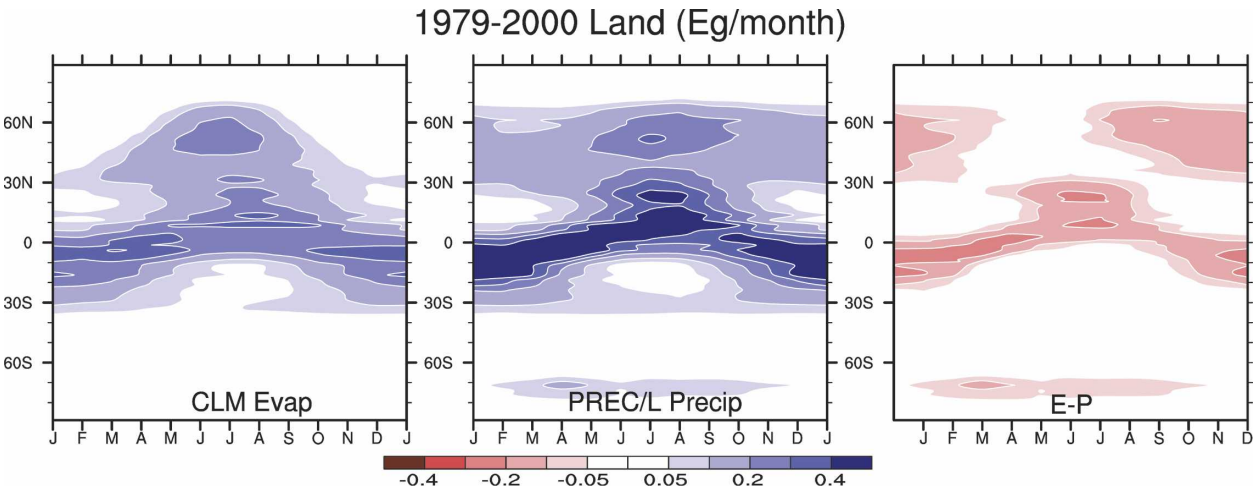

FIG. 7. Zonal mean over land for the mean annual cycle from 1979–2000 for the (left) CLM land evapotranspiration, (middle) PREC/L precipitation, and (right) $E - P$ as the difference between the first two (Eg month^{-1}).

precipitation and moisture availability. Values are relatively small in Australia, and again, a strong balance exists between precipitation and evaporation, and only in summer are there moisture convergences and a surplus runoff component. South America includes much of the Amazon and La Plata basins and features strong moisture convergence in summer, when evaporation is also strong, but with plenty of moisture remaining for streamflow. Not shown is Antarctica, which the computations suggest has almost zero evaporation, and monthly precipitation less than 0.5 Eg, peaking in April.

The results on inferred moisture convergence are at odds with the direct computations of moisture convergence from ERA-40. To show this, we take zonal means over land of the various fields that have gone into these figures (Fig. 7) and contrast them with the results from ERA-40 (Fig. 8). The last panel in each of Figs. 7 and 8 can be directly compared. Note the distinct annual cycle of moisture storage in the atmosphere (Fig. 8), even though the values are not large. In Fig. 7, $P > E$ throughout most of the year, as we expect over land for the annual mean. The only way this could not be true is if there is large storage of moisture on land in one month, which subsequently evaporates in another. Indeed, water storage on land as snow that subsequently melts in spring and replenishes the soil moisture can result in $E > P$ for those months. Results from the Gravity Recovery and Climate Experiment (GRACE) satellite mission based on variations in gravity also sug-

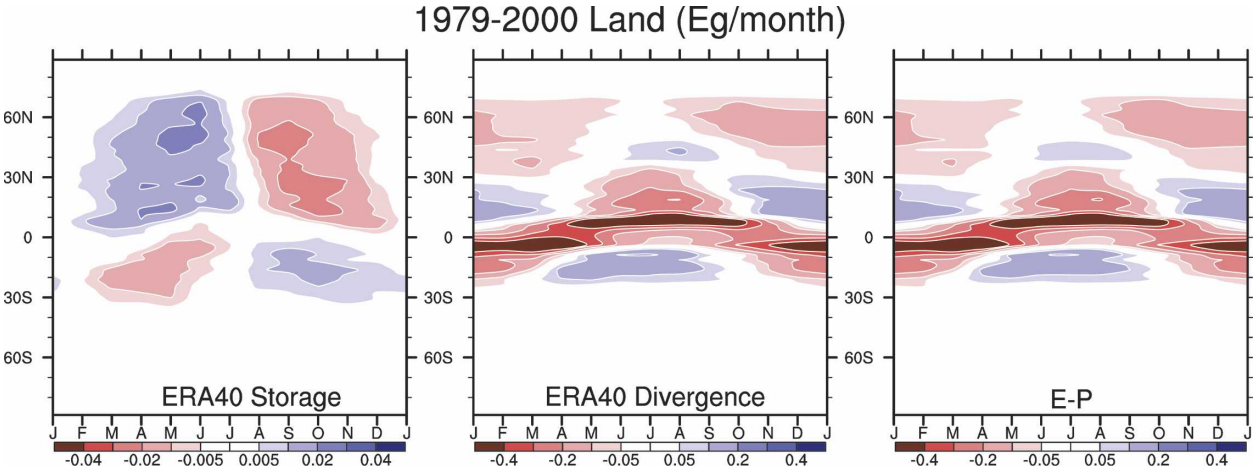

FIG. 8. Annual cycle over land computed from the moisture budget from ERA-40 reanalyses from 1979–2000 of the (left) zonal mean change in atmospheric storage of water vapor, (middle) vertical integral of the divergence of moisture, and (right) their sum as $E - P$ (Eg month^{-1}).

gest substantial annual cycles in water storage on land in lower latitudes, especially in monsoon areas (Wahr et al. 2004), and there is some evidence for this in the results that go into Fig. 7 just south of the equator in May–June, where E exceeds P in the dry season by close to 0.05 Eg, with contributions from the Amazon, Australia, and southern Africa. However, in Fig. 8, both the moisture divergence and $E - P$ are strongly positive in the subtropics of the winter hemisphere. In fact this is true in ERA-40 data over Australia in 9 months of the year as well as for the annual mean, which is clearly not physically possible. Hence the low-level mass divergence associated with subsidence in the downward branch of the monsoon circulations is accompanied by a low-level divergent moisture flux that is not correct in ERA-40. Spurious sources of moisture exist either from surface evaporation that fails to dry out the ground or from increments in the analysis that continually restore the moisture fields to observed levels. Hence the ERA-40 moisture budget is not balanced. The problem is not confined to Australia, but for other continents the divergence in some areas and months is compensated for by convergence elsewhere. Accordingly, much greater credence is given to the last panel in Fig. 7 for the zonal mean $E - P$ over land.

5. Discussion and conclusions

We have presented new estimates of continental land and zonal mean annual cycles of P, E, and $E - P$, and we have further shown the potential for in-depth analysis over land using reanalyses. However, substantial improvements are required in the reanalyses to satisfy the total moisture cycle. The material presented here provides a commentary on the deficiencies in ERA-40 with regard to the hydrological cycle. Major problems are evident throughout the Tropics and subtropics, with evaporation too strong over land in the subtropics, exceeding the actual moisture supply, and precipitation too strong in the monsoon trough and convergence zones. The latter follows from the excessively low $E - P$ values in Fig. 8 relative to Fig. 7, and is consistent with Uppala et al. (2005). Although we used gauge precipitation without bias corrections, and the bias likely leads to an underestimate, these are relatively large only during high-latitude winter and over high terrain.

Much more reliable estimates are available over land from ground-based networks of precipitation and we have used estimates of evapotranspiration from a sophisticated land model driven by realistic forcings. Hence, plausible estimates of evapotranspiration can be made physically consistent with the supply of moisture and runoff, as well as the available energy supply. Nonetheless, comparisons with runoff estimates suggest deficiencies that can probably only be remedied by fully accounting for the variations over time and changes in and reliability of observations over time.

We have also presented a new estimate of the global hydrological cycle (Fig. 1), with the main terms computed from recent data, including precipitation over land and ocean, river discharge into the oceans and thus moisture convergence over land, and estimates of the main reservoirs. These values depend somewhat on the period used for the data, and hence the challenge is to be able to compute this monthly, or more often, for continents, river basins, and watersheds.

Acknowledgments. This research is partially sponsored by the NOAA CLIVAR and CCDD programs under Grants NA17GP1376 and NA04OAR4310073, NSF Grant ATM-0233568, and by the Water Cycle Program at NCAR.

REFERENCES

Adam, J. C., and D. P. Lettenmaier, 2003: Adjustment of global gridded precipitation for systematic bias. *J. Geophys. Res.,* **108,** 4257, doi:10.1029/2002JD002499.

——, E. A. Clark, D. P. Lettenmaier, and E. F. Wood, 2006: Correction of global precipitation products for orographic effects. *J. Climate,* **19,** 15–38.

Adler, R. F., and Coauthors, 2003: The version 2 Global Precipitation Climatology Project (GPCP) monthly precipitation analysis (1979–present). *J. Hydrometeor.,* **4,** 1147–1167.

Alley, W. M., R. W. Healy, J. W. LaBaugh, and T. E. Reilly, 2002: Flow and storage in groundwater systems. *Science,* **296,** 1985–1990.

Baumgartner, A., and E. Reichel, 1975: *The World Water Balance.* Elsevier Scientific, 179 pp.+31 maps.

Bonan, G. B., K. W. Oleson, M. Vertenstein, S. Levis, X. B. Zeng, Y. J. Dai, R. E. Dickinson, and Z. L. Yang, 2002: The land surface climatology of the Community Land Model coupled to the NCAR Community Climate Model. *J. Climate,* **15,** 3123–3149.

Chahine, M. T., 1992: The hydrological cycle and its influence on climate. *Nature,* **359,** 373–380.

Chen, M., P. Xie, J. E. Janowiak, and P. A. Arkin, 2002: Global land precipitation: A 50-yr monthly analysis based on gauge observations. *J. Hydrometeor.,* **3,** 249–266.

Curtis, S., and R. F. Adler, 2003: The evolution of El Niño–precipitation relationships from satellites and gauges. *J. Geophys. Res.,* **108,** 4153, doi:10.1029/2002JD002690.

Dai, A., 2001a: Global precipitation and thunderstorm frequencies. Part I: Seasonal and interannual variations. *J. Climate,* **14,** 1092–1111.

——, 2001b: Global precipitation and thunderstorm frequencies. Part II: Diurnal variations. *J. Climate,* **14,** 1112–1128.

——, 2006: Recent climatology, variability, and trends in global surface humidity. *J. Climate,* **19,** 3589–3606.

——, and K. E. Trenberth, 2002: Estimates of freshwater discharge from continents: Latitudinal and seasonal variations. *J. Hydrometeor.,* **3,** 660–687.

——, and ——, 2003: New estimates of continental discharge and oceanic freshwater transport. *Proc. Symp. on Observing and Understanding the Variability of Water in Weather and Climate,* Long Beach, CA, Amer. Meteor. Soc., CD-ROM, JP1.11.

——, F. Giorgi, and K. E. Trenberth, 1999a: Observed and model-simulated diurnal cycles of precipitation over the contiguous United States. *J. Geophys. Res.,* **104,** 6377–6402.

——, K. E. Trenberth, and T. R. Karl, 1999b: Effects of clouds, soil moisture, precipitation, and water vapor on diurnal temperature range. *J. Climate,* **12,** 2451–2473.

——, ——, and T. Qian, 2004: A global data set of Palmer Drought Severity Index for 1870–2002: Relationship with soil moisture and effects of surface warming. *J. Hydrometeor.,* **5,** 1117–1130.

——, T. R. Karl, B. Sun, and K. E. Trenberth, 2006: Recent trends in cloudiness over the United States: A tale of monitoring inadequacies. *Bull. Amer. Meteor. Soc.,* **87,** 597–606.

Daly, C., W. P. Gibson, G. H. Taylor, G. L. Johnson, and P. Pasteris, 2002: A knowledge based approach to the statistical mapping of climate. *Climate Res.,* **22,** 99–113.

Dickinson, R. E., K. W. Oleson, G. B. Bonan, F. Hoffman, P. Thornton, M. Vertenstein, Z.-L. Yang, and X. Zeng, 2006: The Community Land Model and its climate statistics as a component of the Community Climate System Model. *J. Climate,* **19,** 2302–2324.

Dozier, J., 1992: Opportunities to improve hydrological data. *Rev. Geophys.,* **30,** 315–331.

Fasullo, J., and D. Z. Sun, 2001: Radiative sensitivity to water vapor under all-sky conditions. *J. Climate,* **14,** 2798–2807.

Gleick, P. H., 1993: *Water in Crisis: A Guide to the World's Fresh Water Resources.* Oxford University Press, 504 pp.

Groisman, P. Ya., R. W. Knight, D. R. Easterling, T. R. Karl, G. C. Hegerl, and V. N. Razuvaev, 2005: Trends in intense precipitation in the climate record. *J. Climate,* **18,** 1326–1350.

Houghton, J. T., Y. Ding, D. J. Griggs, M. Noguer, P. J. van der Linden, X. Dai, K. Maskell, and C. A. Johnson, Eds., 2001: *Climate Change 2001: The Scientific Basis*. Cambridge University Press, 881 pp.

Karl, T. R., and K. E. Trenberth, 2003: Modern global climate change. *Science,* **302,** 1719–1723.

Kiehl, J. T., and K. E. Trenberth, 1997: Earth's annual global mean energy budget. *Bull. Amer. Meteor. Soc.,* **78,** 197–208.

Korzun, V. I., 1978: *World Water Balance and Water Resources of the Earth*. Studies and Reports in Hydrology, Vol. 25, UNESCO, 587 pp.

Mitchell, T. D., and P. D. Jones, 2005: An improved method of constructing a database of monthly climate observations and associated high-resolution grids. *Int. J. Climatol.,* **25,** 693–712.

Ohmura, A., 2004: Cryosphere during the twentieth century. *The State of the Planet, Geophys. Monogr.,* Vol. 150, Amer. Geophys. Union, 239−257.

Oki, T., 1999: The global water cycle. *Global Energy and Water Cycles,* K. A. Browning and R. J. Gurney, Eds., Cambridge University Press, 10–29.

Peixoto, J. P., and A. H. Oort, 1992: *Physics of Climate*. American Institute of Physics, 520 pp.

Qian, T., A. Dai, K. E. Trenberth, and K. W. Oleson, 2006: Simulation of global land surface conditions from 1948 to 2004: Part I: Forcing data and evaluations. *J. Hydrometeor.,* **7,** 953–975.

Schlesinger, W. H., 1997: *Biogeochemistry: An Analysis of Global Change*. 2d ed. Academic Press, 588 pp.

Shiklomanov, I. A., 1993: World fresh water resources. *Water in Crisis: A Guide to the World's Fresh Water Resources,* P. H. Gleick, Ed., Oxford University Press, 13–24.

——, and J. C. Rodda, Eds., 2003: *World Water Resources at the Beginning of the Twenty-First Century.* International Hydrology Series, Cambridge University Press, 435 pp.

Soden, B. J., D. L. Jackson, V. Ramaswamy, D. Schwarzkopf, and X. Huang, 2005: The radiative signature of upper tropospheric moistening. *Science,* **310,** 841–844.

Trenberth, K. E., 1998: Atmospheric moisture residence times and cycling: Implications for rainfall rates with climate change. *Climatic Change,* **39,** 667–694.

——, 1999: Atmospheric moisture recycling: Role of advection and local evaporation. *J. Climate,* **12,** 1368–1381.

——, and C. J. Guillemot, 1998: Evaluation of the atmospheric moisture and hydrological cycle in the NCEP/NCAR reanalyses. *Climate Dyn.,* **14,** 213–231.

——, and D. P. Stepaniak, 2003a: Co-variability of components of poleward atmospheric energy transports on seasonal and interannual timescales. *J. Climate,* **16,** 3691–3705.

——, and ——, 2003b: Seamless poleward atmospheric energy transports and implications for the Hadley circulation. *J. Climate,* **16,** 3706–3722.

——, and D. J. Shea, 2005: Relationships between precipitation and surface temperature. *Geophys. Res. Lett.,* **32,** L14703, doi:10.1029/2005GL022760.

——, and L. Smith, 2005: The mass of the atmosphere: A constraint on global analyses. *J. Climate,* **18,** 864–875.

——, J. M. Caron, and D. P. Stepaniak, 2001: The atmospheric energy budget and implications for surface fluxes and ocean heat transports. *Climate Dyn.,* **17,** 259–276.

——, A. Dai, R. M. Rasmussen, and D. B. Parsons, 2003: The changing character of precipitation. *Bull. Amer. Meteor. Soc.,* **84,** 1205–1217.

——, J. Fasullo, and L. Smith, 2005: Trends and variability in column integrated atmospheric water vapor. *Climate Dyn.,* **24,** 741–758.

Uppala, S. M., and Coauthors, 2005: The ERA-40 reanalysis. *Quart. J. Roy. Meteor. Soc.,* **131,** 2961–3012.

Wahr, J., S. Swenson, V. Zlotnicki, and I. Velicogna, 2004: Time-variable gravity from GRACE: First results. *Geophys. Res. Lett.,* **31,** L11501, doi:10.1029/2004GL019779.

Webb, R. S., C. E. Rosenzweig, and E. R. Levine, 1993: Specifying land surface characteristics in general circulation models: Soil profile data set and derived water holding capacities. *Global Biogeochem. Cycles,* **7,** 97–108.

Xie, P., and P. A. Arkin, 1997: Global precipitation: A 17-year monthly analysis based on gauge observations, satellite estimates and numerical model outputs. *Bull. Amer. Meteor. Soc.,* **78,** 2539–2558.

Yang, D. Q., D. Kane, Z. P. Zhang, D. Legates, and B. Goodison, 2005: Bias corrections of long-term (1973–2004) daily precipitation data over the northern regions. *Geophys. Res. Lett.,* **32,** L19501, doi:10.1029/2005GL024057.

Yin, X. G., A. Gruber, and P. Arkin, 2004: Comparison of the GPCP and CMAP merged gauge-satellite monthly precipitation products for the period 1979–2001. *J. Hydrometeor.,* **5,** 1207–1222.

Zhang, T., R. G. Barry, K. Knowles, J. A. Heginbottom, and J. Brown, 1999: Statistics and characteristics of permafrost and ground ice distribution in the Northern Hemisphere. *Polar Geogr.,* **23** (2), 132–154.